https://ntrs.nasa.gov/search.jsp?R=20170005523 2019-05-01T03:49:48+00:00Z

Chromospheric LAyer SpectroPolarimeter (CLASP2)

Noriyuki Narukage[a], Jonathan W. Cirtain[b], Ryoko Ishikawa[a], Javier Trujillo-Bueno[c], Bart De Pontieu[d], Masahito Kubo[a], Shin-nosuke Ishikawa[e], Ryouhei Kano[a], Yoshinori Suematsu[a], Masaki Yoshida[a], Ken Kobayashi[b], Amy R. Winebarger[b], Andres Asensio Ramos[c], Tanausu del Pino Aleman[c], Jiri Štěpán[f], Luca Belluzzi[g], Juan Ignacio Larruquert[h], Frédéric Auchère[i], Jorrit Leenaarts[j], and Mattias J. L. Carlsson[k]

[a]National Astronomical Observatory of Japan, 2-21-1 Osawa, Mitaka, Tokyo, JAPAN, 181-8588
[b]NASA Marshall Space Flight Ctr., Address, City, Country
[c]Instituto de Astrofísica de Canarias, Address, City, Country
[d]Lockheed Martin Space Systems Co., Address, City, Country
[e]Institute of Space and Astronautical Science/Japan Aerospace Exploration Agency, Address, City, Country
[f]Astronomical Institute of the ASCR, v.v.i., Address, City, Country
[g]Istituto Ricerche Solari Locarno, Address, City, Country
[h]Consejo Superior de Investigaciones Científicas, Address, City, Country
[i]Institut d'Astrophysique Spatiale, Address, City, Country
[j]Stockholm Univ., Address, City, Country
[k]Univ. I Oslo, Address, City, Country

ABSTRACT

The sounding rocket Chromospheric Lyman-Alpha SpectroPolarimeter (CLASP) was launched on September 3rd, 2015, and successfully detected (with a polarization accuracy of 0.1 %) the linear polarization signals (Stokes Q and U) that scattering processes were predicted to produce in the hydrogen Lyman-alpha line (Lyα; 121.567 nm). Via the Hanle effect, this unique data set may provide novel information about the magnetic structure and energetics in the upper solar chromosphere. The CLASP instrument was safely recovered without any damage and we have recently proposed to dedicate its second flight to observe the four Stokes profiles in the spectral region of the Mg II h and k lines around 280 nm; in these lines the polarization signals result from scattering processes and the Hanle and Zeeman effects. Here we describe the modifications needed to develop this new instrument called the "Chromospheric LAyer SpectroPolarimeter" (CLASP2).

Keywords: UV spectropolarimetry, Chromospheric magnetic field, Hanle effect, Zeeman effect, CLASP project, sounding rocket experiment

1. INTRODUCTION

Recent observational advances enabled by the Hinode/Solar Optical Telescope (SOT) and the Interface Region Imaging Spectrometer (IRIS) have revolutionized our view of the highly dynamic upper solar chromosphere and the critical role this interface region between the photosphere and corona plays in the mass and energy balance of the outer solar atmosphere. A major remaining challenge for heliophysics is to decipher the magnetic structure of the solar chromosphere. The importance of measuring the chromospheric magnetic field is due to both the key role the chromosphere plays in energizing and structuring the outer solar atmosphere and the inability of extrapolation of photospheric fields to adequately describe this boundary region, which is key to understanding what drives instabilities in the solar atmosphere (e.g., flares and coronal mass ejections). Progress toward these

Further author information: (Send correspondence to Noriyuki Narukage)
Noriyuki Narukage: E-mail: noriyuki.narukage@nao.ac.jp

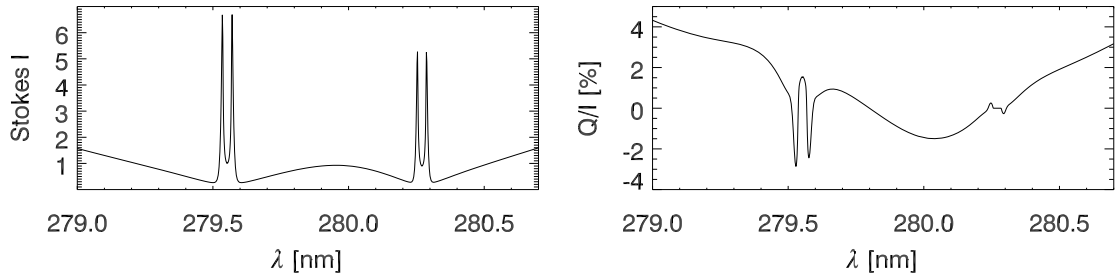

Figure 1. The Stokes I profiles (left panel; units: $10^{17}\times$ Number of Photons $\mathrm{cm}^{-2}\,\mathrm{s}^{-1}\mathrm{sr}^{-1}\mathrm{nm}^{-1}$), and the Q/I scattering polarization pattern (right panel) of the Mg II h & k lines calculated in a semi-empirical model of the quiet solar atmosphere for a close to the limb line of sight ($\mu = \cos\theta = 0.1$, with θ the heliocentric angle). The positive reference direction for Stokes Q is the parallel to the nearest limb.

goals requires 1) identifying observables sensitive to the magnetic fields of the upper chromosphere and transition region, 2) developing diagnostic tools to infer the magnetic fields from the observables, and 3) designing and building the instrumentation needed to measure the observables. Over the last few years, significant progress has been made in the first two tasks providing the required theoretical background for new instrumentation.

Most of the magnetically sensitive spectral line radiation emitted in the transition region is in the ultraviolet spectrum, necessitating observations above the absorbing terrestrial atmosphere to measure their Stokes I, Q, U and V profiles (of which Q, U and V encode the magnetic field information). In September 2015, the Chromospheric Lyman-Alpha Spectro-Polarimeter (CLASP) will be launched from White Sands Missile Range. CLASP will achieve the first measurement of the linear polarization produced by scattering processes in a far UV resonance line (hydrogen Lyman-α) and the first exploration of the magnetic field in quiet regions of the chromosphere-corona transition region. Lyman-α, however, is only one of the magnetically sensitive spectral lines in the UV spectrum; the magnetically sensitive Mg II k spectral line near 280 nm, whose core forms only about 100 km below the Lyman-α core, is probably an even more compelling target.[1] This is because, in addition to being sensitive to the Hanle effect, the Mg II k line is predicted to show measurable circular Zeeman polarization signals for field strengths as low as 50 G. Studying this line is particularly timely since its intensity spectrum has been extensively studied over the past few years with high-resolution IRIS observations and advanced numerical models.

We propose the Chromospheric LAyer Spectro-Polarimeter 2 (CLASP2). We will refit the existing CLASP instrument for observing the wavelength variation of the four Stokes parameters in the 280 nm range, due to the anisotropic radiation pumping and the Hanle and Zeeman effects. Both CLASP1 and 2 serve as pathfinders for potential satellite missions to measure the magnetic field in the upper chromosphere and transition region of our nearest star.

2. METHODOLOGY OF EXPLORATION OF MAGNETIC FIELDS IN THE UPPER CHROMOSPHERE AND THE TRANSITION REGION

2.1 The Hanle and Zeeman Effect in Mg II h & k for Probing the Magnetism of the Upper Chromosphere

The hydrogen Lyman-α line at 121.6 nm and the Mg II k line at 279.5 nm are of great scientific interest because their line-center signals are formed in the chromosphere and transition region and because their polarization signals have an interesting magnetic sensitivity.[1–5] Each of these spectral lines is sensitive to the Hanle effect, which is the magnetic field-induced modification of the linear polarization produced in a spectral line by the absorption and scattering of anisotropic radiation.[6] While the Hanle effect in Lyman-α is sensitive to magnetic fields with strengths $10 \lesssim B \lesssim 100$ gauss, the Hanle effect in the Mg II k line can be exploited to detect even weaker fields (with $5 \lesssim B \lesssim 50$ gauss). In addition, while the contribution of the Zeeman effect to the circular (Stokes V) and linear polarizations of the Lyman-α line is predicted to be insignificant, it is expected to be measurable in the Mg II h and k lines.

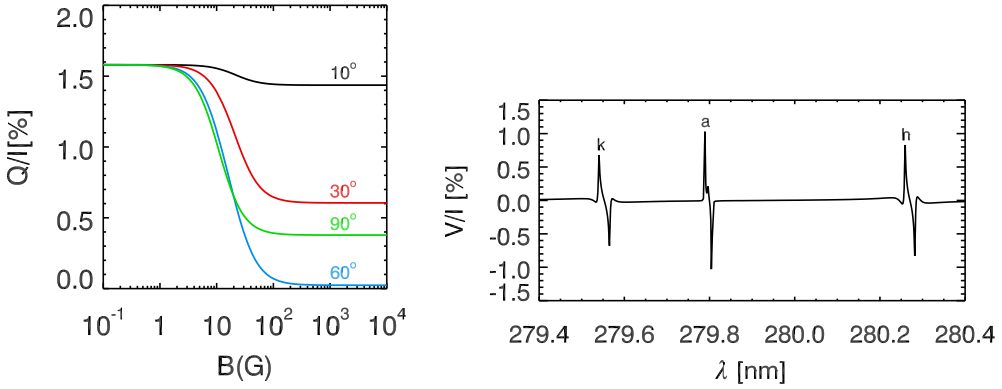

Figure 2. Left panel: illustration of the Hanle effect at the center of the Mg II k line for a LOS with $\mu = 0.1$. It results from radiative transfer calculations in a semi-empirical model of the quiet solar atmosphere, assuming that it is permeated by a random-azimuth magnetic field with the indicated inclination with respect to the solar local vertical. Right panel: theoretical V/I profiles due to a 50 G longitudinal field. In addition to the k line at 279.55 nm and the h line at 280.27 nm, we show also the circular polarization signal in the (blended) subordinate line of Mg II whose lower level is the upper level of the k resonance line (i.e., the line labelled "a").

The Chromospheric Lyman-α Spectro-Polarimeter (CLASP) has been designed to measure the Stokes I, Q and U profiles of the hydrogen Lyman-α line in quiet regions of the solar disk. With only two observables sensitive to the magnetic field (Q/I and U/I) it is not possible to determine the three components of the magnetic field vector. For this reason, the CLASP1 observations will be complemented with other ground-based and space observations with the aim of constraining the azimuth of the magnetic field in the observed region.[7] Measuring in addition the Stokes V signal would determine the magnetic field vector directly from the spectropolarimetric observations. For this reason, the second flight of CLASP aims at measuring the Stokes V signals in the spectral region of the Mg II h & k resonance lines, in addition to their Stokes I, Q and U profiles.

The left and right panels of Figure 1 show the Stokes I and Q/I patterns of the Mg II h and k lines resulting from detailed radiative transfer calculations in a semi-empirical model of the quiet solar atmosphere. These calculations account for the important effects due to partial frequency redistribution (PRD) and quantum interference between the upper J-levels of the h and k lines and include the interaction between the line scattering processes and those responsible of the polarization of the Sun's continuous radiation. In the line wings the Q/I polarization amplitudes are of the order of a few percent (see Ref. 1). At the center of the k line the Q/I signal is of the order of 1%, while $Q/I = 0$ at the very center of the (intrinsically unpolarizable) h line. The Hanle effect operates at the center of the k line, and by measuring simultaneously the scattering polarization pattern across the Mg II h & k lines we will have automatically a way to fix the zero offset of the polarization scale.

Left panel of Figure 2 shows the sensitivity to the Hanle effect of the scattering polarization at the center of the Mg II k line, calculated for a close to the limb LOS in a semi-empirical model of the quiet solar atmosphere for various inclinations of the imposed random-azimuth magnetic field. The impact of the Zeeman effect on the circular polarization (Stokes V) of the Mg II lines is illustrated in the right panel of Figure 2. Interestingly, for a longitudinal field of 50 G the Zeeman effect produces V/I signals of about 0.5% in the Mg II resonance lines, as well as in the subordinate line "a" located between the h & k lines.

In conclusion, with the second flight of CLASP we aim at measuring the wavelength variation of the four Stokes parameters in the spectral region between 279.4 nm and 280.4 nm, where we have several Mg II lines sensitive to the physical conditions of the solar chromosphere through a diagnostically important range of heights, including the upper chromosphere just below the enigmatic transition region.

2.2 Scientific Requirements

Observing the scattering polarization across the Mg II h & k lines and detecting the Hanle effect at the core of the k line are the primary goals for the second flight of CLASP. The second objective is to detect the circular polarization caused by the Zeeman effect in the Mg II h & k lines. By interpreting the observed linear (Q/I and U/I) and circular (V/I) polarization profiles, information on the vector magnetic field can then be inferred. While the simple weak field approximation can be applied to the Zeeman V/I signals to obtain estimations of the longitudinal component of the magnetic field, the interpretation of the Q/I and U/I line-core signals requires detailed radiative transfer modeling of the observed polarization. We will do this by applying recently-developed radiative transfer tools[8,9] and the increasingly realistic 3D solar atmospheric models developed by the Oslo group. In this section, we discuss the scientific requirements of the proposed instrument to achieve the above-mentioned measurements, summarized in Table 1.

Table 1. Summary of Scientific Requirements

Observable	Requirement
Target	On-disk, away from disk center (Quiet Sun and other structures)
Polarization Sensitivity	0.1% (line core of Mg II h and k)
Spectroscopic Resolution	0.025 nm
Spectral Window	279.4 − 280.4 nm
Spatial Resolution	2−3″
Temporal Resolution	< 5 minutes

2.2.1 Target Selection

The theoretical predictions suggest that the most appropriate targets are on-disk regions located away from the solar disk center, in order to maximize the chances of detecting the linear polarization due to scattering processes, along with its modification by the Hanle effect. Similar to the first flight, we aim at probing the quiet Sun magnetism in the upper chromosphere, which has barely been investigated before. However, the CLASP2 measurements will be the first measurements of Stokes I, Q, U *and* V, allowing full vector magnetometry in the upper chromosphere for the first time. To this end, we will put the 400 arcsec long slit oriented perpendicular to the limb and with one of its extremes located at 20 arcsec off the limb. This will allow us to measure the center-to-limb (CLV) variation of the Stokes profiles, an information suitable to constrain the temperature stratification of the observed atmospheric region.[5] In addition, the slit will ideally cross plage regions if they are available, since we expect field strengths of > 50 G to occur in plage. It is also important to address the question of how mixed the polarities are within plage (which has an impact on jet formation[10]).

2.2.2 Polarization Sensitivity

The measurement sensitivity requirements are based on reported estimates of the field strength in some chromospheric structures, as well as on theoretical estimates. In quiet Sun spicules, magnetic fields as strong as ~ 50 G have been detected.[11] Concerning the theoretical results on the Hanle effect presented in the left panel of Figure 2, spectropolarimetric measurements with a sensitivity of 0.1% will be necessary. With this polarization sensitivity and a spectral resolution of 0.025 nm (Section 2.2.3) we should be able to detect longitudinal magnetic fields as low as 50 G via the Zeeman effect. Hence, we require 0.1% polarimetric sensitivity at the line core of the Mg II h and k lines.

2.2.3 Spectroscopic Resolution

We have considered the impact of the spectral resolution on the polarization signatures by convolving the calculated Stokes profiles with gaussian functions of different widths. In order to detect the line-core Q/I and U/I signals without a significant deterioration and to detect the antisymmetric V/I signals, a spectral resolution of at least 0.025 nm is required (Figure 3). This wavelength resolution can be achieved without a significant modification of CLASP1 instrument.

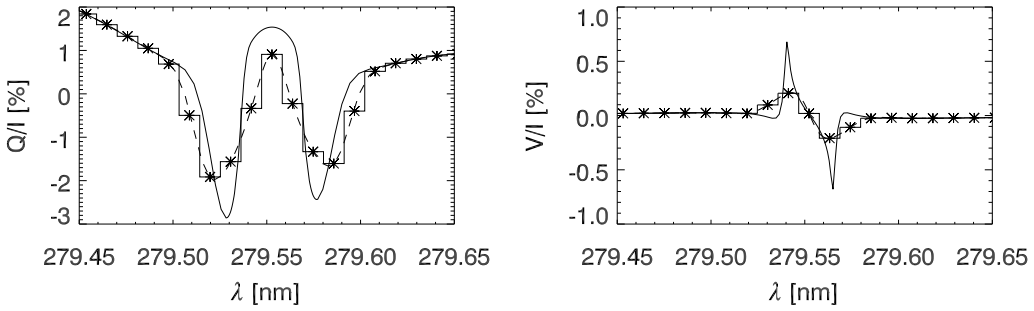

Figure 3. *Left:* Theoretical estimate of the Q/I signals in Mg II k (for a on-disk observation close to the limb) produced by scattering processes in the solar transition region. *Right:* The wavelength variation of V/I around the Mg II k line, taking into account the Zeeman effect of a longitudinal magnetic field of 50 G. The solid lines correspond to the pure theoretical solution without any spectral smearing. Dashed curves include the effect of spectral smearing by convolving with a Gaussian of FWHM of 0.018 nm (PSF estimated from CLASP1 performance, see Section **??**). The asterisks consider a spectral sampling of 0.011 nm/pix (Figure 5), resulting in an effective wavelength resolution of 0.022 nm (Nyquist limited).

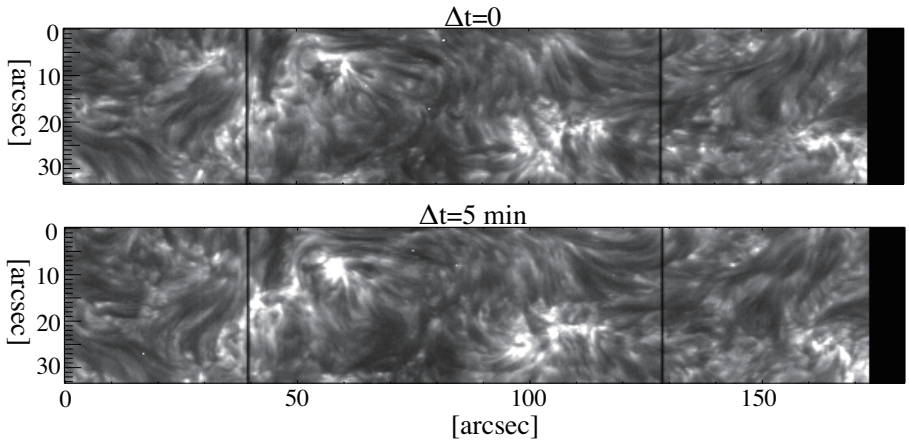

Figure 4. Images of the quiet Sun disk separated by a 5 minutes interval taken with IRIS at the core of the Mg II h & k lines.

2.2.4 Spectral Window

The Mg II lines we are interested in are the h and k resonance lines as well as the subordinate line "a" located between them (see right panel of Figure 2). Thus, we require a wavelength window of 279.4−280.4 nm. Measuring the Stokes profiles of all these lines simultaneously will give us precious information on an important range of heights in the solar chromosphere.

2.2.5 Spatial and Temporal Resolution

Clearly, the upper chromosphere is a very dynamic region with rapid variations of density and temperature on small scales and physical conditions that vary between adjacent field lines. However, the rapid changes in the thermodynamics are not necessarily associated by equally large fluctuations in the magnetic field. The magnetic structure in the upper chromosphere is very likely relatively simple, being almost force-free.[12] Here we use the typical length scales and lifetimes of structures as a proxy for the required resolution.

Mg II h and k line core images of the quiet Sun (see Figure 4) reveal the existence of thin threads with thicknesses of 2−3″ and lengths of 10″− 20″. Additionally, we have found that the change in intensity in the threads is very little over a 5-minute window.

3. TECHNICAL APPROACH

3.1 Instrument Design

CLASP2 is a spectropolarimeter optimized for observing the Mg II line around 280 nm without significant modification of CLASP1 optical design.[13] The instrument is composed of a Cassegrain telescope, a rotating wave plate, a dual-beam spectrograph assembly with a grating working as a beam splitter, an identical pair of reflective polarization analyzers each equipped with a CCD camera, and a slitjaw imaging system. The overall layout and baseline design parameters are shown in Figure 5.

3.1.1 Structural Design

The mechanical structure from the first flight of CLASP (Figure 5) is mostly reused for CLASP2. The telescope and spectrograph are assembled as separate structures, allowing each section to be optically aligned independently before integration and end-to-end system alignment. Each section is cantilevered from the main interface plate which attaches to the rocket skin.

3.1.2 Telescope

After the successful flight of CLASP1, the primary mirror will be recoated for best reflectance at 280 nm. The telescope design defines the aperture by an aperture stop at the telescope entrance, sized to prevent sunlight from illuminating the telescope structures surrounding the primary mirror. The primary mirror uses a "cold mirror" coating, i.e. a narrowband multilayer coating that reflects the target wavelength but is transparent to visible light. As shown in Figure 5 schematic, this allows most of the visible light to pass through the primary mirror and onto the heat absorber, which is thermally isolated from the telescope and spectrograph. With the CLASP1 instrument, we confirmed that this reduced the heat load on subsequent optical components and minimized the visible light in the spectrograph and slit-jaw system (Section 3.3). Our baseline is dual-bandpass cold mirror coating of Mg II h & k lines for the spectropolarimeter and Lyman-α line for the slitjaw system (Section 3.1.5). Such dual-band cold mirror coating has been used on the MSFC Solar Ultraviolet Magnetograph Instrument (SUMI) sounding rocket experiment[14] and IRIS.[15] The expected coating performance is shown in Figure 6.

3.1.3 Polarimeter System

The polarimeter system consists of a rotating wave plate and two reflective polarization analyzers (Figure 5). The rotating waveplate (Section 3.1.3) allows measurement of Stokes Q, U, and V with fixed polarization analyzers. The optical components between the waveplate and polarization analyzers are oriented to minimize polarization errors and crosstalk: the ruling of the diffraction grating is parallel to the polarization axes of the polarizers, and the camera mirrors are tilted around the same axis. These configurations were adopted for CLASP1, and it was verified that they ensure minimum polarization crosstalk by an end-to-end polarization calibration of the spectropolarimeter system.[16]

The design and performance of the polarimeter system are strongly dependent on the optical properties of materials and coatings at the wavelengths of Mg II h & k. Therefore a comprehensive testing program using the Ultraviolet Synchrotron Orbital Radiation Facility (UVSOR) at the Institute for Molecular Sciences, an affiliated institute of the National Astronomical Observatory of Japan (NAOJ), has been initiated to make measurements on optical material samples, and flight components. This performance characterization validation and testing program has been a continuous effort since the beginning of the CLASP1 development program (e.g., Ref. 17).

MgF_2 Waveplate The waveplate is a compound zero-order waveplate consisting of two stacked MgF_2 plates with slightly different thicknesses and their principal axes rotated by 90° from each other. Using the birefringence in Ref. 18, the phase retardation of the CLASP2 flight waveplate is designed to be 127° to equally measure Q, U, and V. It will be provided by the same vender who fabricated the CLASP1 flight waveplate, and tested before integration at UVSOR. The sophisticated procedure to measure the phase retardation was established as a result of our effort to precisely measure the birefringence of MgF_2 around the Lyman-α line[19] and directly applicable to the new wavelengths of interest.

We reuse the waveplate rotation mechanism which is a hollow DC brushless motor developed by Mitsubishi Precision Co, Ltd. and is designed specifically for the continuous rotation. We confirmed that the rotation speed

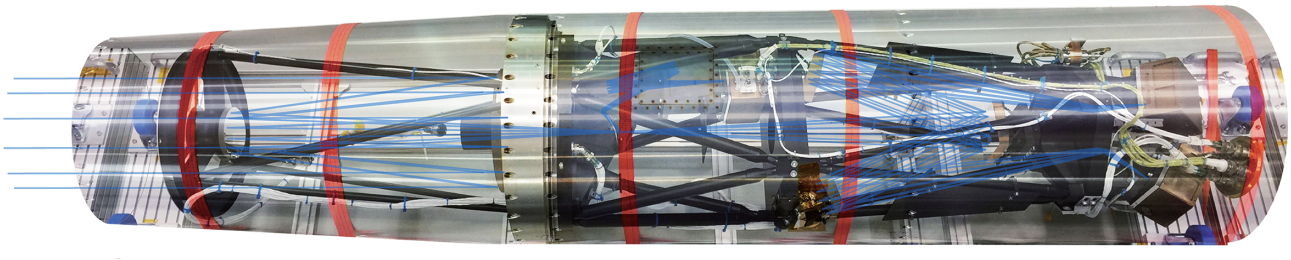

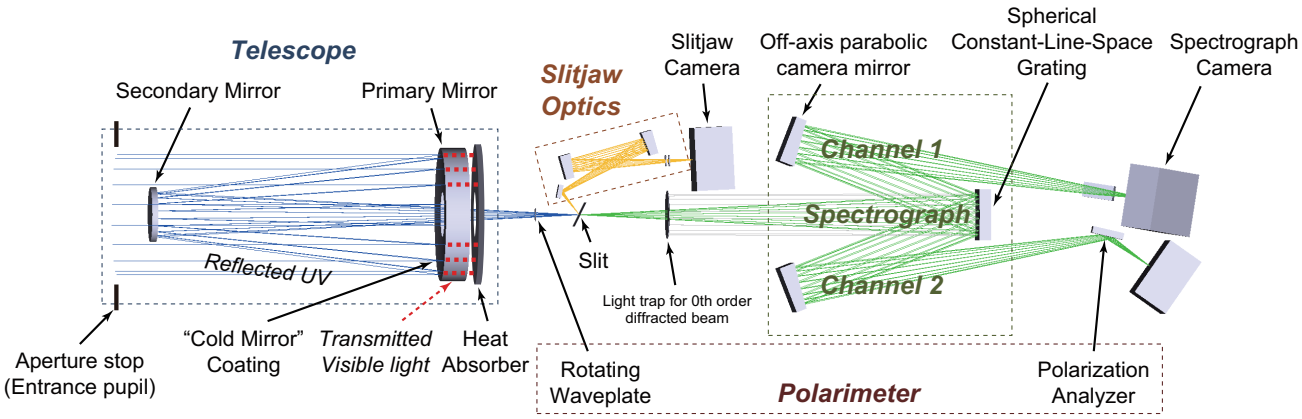

Telescope	
Type	Cassegrain
Aperture	ø277.4 mm
Eff. Focal Length	2614 mm (F/9.42)
Primary Mirror	ø290 mm (clear aperture), F/3.54
Secondary Mirror	ø119.4 mm
Visible Light Rejection	"Cold Mirror" coating on primary mirror

Slit	
Slit Width	18.4 µm (1.45 arcsec)
Slit Length	5.1 mm (400 arcsec)

Slitjaw Imaging System	
Wavelength	Lyα (band-pass filter)
Optics	- Fold mirror with multilayer coating - Off-axis parabola x 2 - Lyα filter x 2
Detector	512 x 512 CCD, 13µm pixel
Plate Scale	1.03 arcsec / pixel
Resolution	2.9 arcsec (spot RMS diameter)
FOV	527 arcsec x 527 arcsec

Polarimeter	
Measurements	Stokes I, Q, U, V
Capability	Simultaneous measurement of orthogonal polarizations
Optics	- Rotating waveplate - Polarization analyzer x 2

Spectrograph	
Spectrograph Type	Inverse Wadsworth mounting
Grating Type	Spherical constant-line-space with 1303 mm^{-1} groove density
Grating Size	ø106 mm (clear aperture)
Wavelength	Optimized for MgII h&k (280 nm)
Camera Mirror	Off-axis parabola
Resolution	0.025 nm (spectral; RMS diameter) 2.2 arcsec (spatial; RMS diameter)
Magnification	0.93

Spectrograph Cameras	
Detector	512 x 512 CCD, 13µm pixel
Exposure Time	0.1 sec (nominal)
Plate Scale	0.011 nm / pixel (spectral) 1.1 arcsec / pixel (spatial)
Field of View	279.4 - 280.4 nm (spectral) 400 arcsec (along slit)

Figure 5. CLASP1 instrument that will be reused for CLASP2 (top), CLASP2 optical layout (middle), and specifications for CLASP2 (bottom).

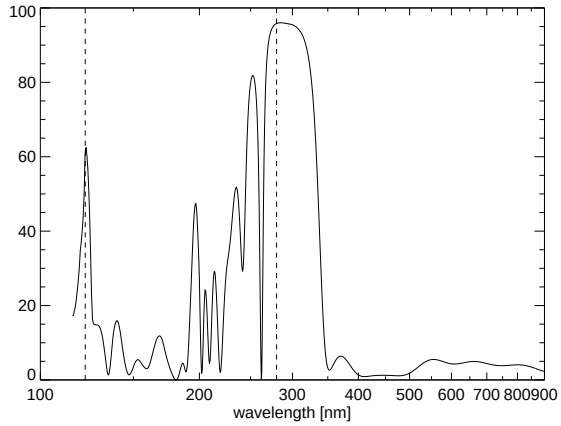

Figure 6. Estimated reflectivity of cold mirror coating on the primary mirror by Acton Optics & Coatings, which reduces the visible light throughput to under 5%. The two dashed lines indicate our target wavelengths of 121.6 nm (Lyman-α) for slitjaw system and 280 nm (Mg II h & k) for spectrograph.

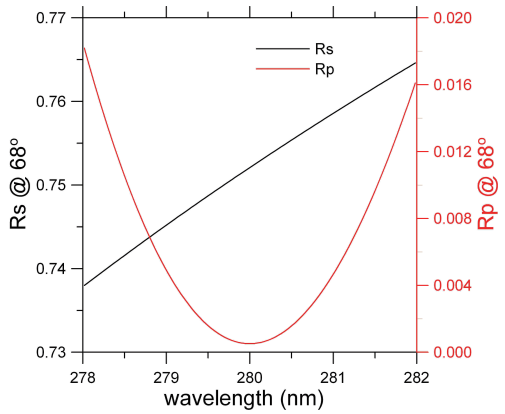

Figure 7. Our estimation of reflectivities of a multilayer-polarization-analyzer sample as a function of incident angle: R_s and R_p for s- and p-polarized lights, respectively.

is so stable that the measurement error of the degree of polarization (i.e., scale error) caused by the rotation non-uniformity is sufficiently small (<0.01%, Ref. 20).

Reflective Polarization Analyzers In the CLASP1 spectropolarimeter, we have employed the polarization analyzer with multi-layer coating based on Ref. 21, which provides us with both high polarization efficiency and high reflectivity at the Lyman-α line. Thus, for the CLASP2, we will use similar polarization analyzers optimized for Mg II h & k lines. This design achieves maximum polarizing efficiency at an incident angle of 68°, which angle is same as that for CLASP1 (Figure 7). The two analyzers are placed at this angle and mounted 90 degrees from each other (with respect to the optical axis) to measure two orthogonal polarizations simultaneously; one is parallel to the ruling direction of the grating, and the other is perpendicular to it. A prototype will be fabricated and tested to optimize the flight coating performance.

3.1.4 Spectrograph

The spectrograph is an inverse Wadsworth configuration using a spherical constant-line-space grating [**?**, Figure 5,]]2015ApOpt..54.2080N with a minimum modification from the CLASP1 spectrograph. The grating disperses the incident beam into the ±1st order collimated beams symmetrically. Each beam is focused on a CCD camera with an off-axis parabolic camera mirror (Figure 8).

A new grating will be fabricated for CLASP2, with the same radius of curvature, but with a ruling density of 1303 lines mm^{-1}. By choosing these parameters, dispersed beams are fed into the off-axis parabolic mirrors as is the case for CLASP1, and we reuse the structure and remaining optical components (i.e., slit, off-axis parabola mirrors and CCDs).

3.1.5 Slitjaw System

The slitjaw system will remain unchanged from the first flight: a Lyman-α imaging system will confirm targeting during flight, facilitate the interpretation of the data obtained by the spectropolarimeter, and obtain context images to be used for co-alignment with other observations. Since IRIS can obtain 2D images with higher spatial and temporal resolutions in the Mg II wavelength range, a Mg II imaging system is not necessary in CLASP2. By keeping the Lyman-α passband in slitjaw system and combining with the IRIS slitjaw observations, we can simultaneously explore the two atmospheric layers in upper chromosphere. Specifications are shown in Figure 5.

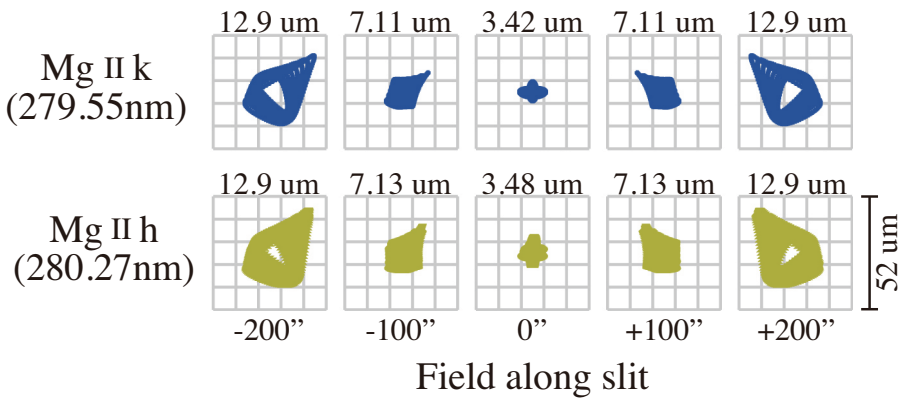

Figure 8. Spot diagrams obtained with the CLASP2 spectrograph in channel 1. The horizontal and vertical panels show the variation in field along the slit and wavelength, respectively. The values above each panel show the spot RMS radii. The full size of each grid is 52 μm (4 pixels), which corresponds to 4.4 arcsec in the spatial direction and 0.044 nm in the spectral dispersion direction. The spot diagrams in channel 2 are horizontal reversals of these.

3.1.6 Spectrograph Detectors

CLASP2 will reuse the existing CLASP1 cameras, developed by MSFC specifically for CLASP1. The cameras use back-thinned e2v CCD57-10 frame-transfer CCDs with Lumogen-E coating for UV sensitivity.

The spectrograph cameras operate in externally triggered frame-transfer mode, synchronized by the trigger signal from the waveplate controller. The trigger signal causes each camera to transfer the image to the storage region and start readout; this also starts the next exposure. The images are read out through 2 readout taps at 500 kilopixels per second per port. In CLASP1, the requirement was 512×256 region-of-interest (ROI) readout at 300 ms cadence. We exceeded this requirement, and will read out 512×384 pixels at this cadence. For CLASP2, the cameras will be operated at 512×128 ROI at 100 ms cadence. SpaceWire interface is used for control and data transfer.

Each camera incorporates an LN2 cooled cold block and a CCD heater. The cold block is cooled by LN2 until the moment of launch, and serves as a thermal reservoir during flight. Each camera cold block is fed through a separate LN2 feedthrough, and the LN2 flow rate is independently and automatically controlled. The CCD heater is controlled by a PID temperature controller which operates throughout flight; it has successfully demonstrated the ability to maintain every CCD at -20 ± 0.1 C for the duration of the flight, and through extended laboratory calibration tests.

For CLASP1, the readout noise requirement for the camera was 25 e- rms, based on allocation within the total error budget for polarization measurement. We greatly surpassed this requirement, and all CLASP1 cameras demonstrated readout noise levels below 6 e- rms.

3.2 Polarization Measurement

3.2.1 Modulation

The observing mode consists of rotating the waveplate at a constant rate and acquiring 16 exposures per waveplate rotation. The waveplate controller electronics creates trigger pulses for the spectropolarimeter cameras with its master clock, insuring synchronization between waveplate rotation and exposure. Based on our estimation of the shortest exposure time to readout out 512(spatial) $\times$ 128(spectral) pixels covering the required wavelength window, the exposure time will be 0.1 sec, resulting in a waveplate rotation period of 1.6 sec.

The observed signal in each spectropolarimeter channel, as a function of time, are:

$t =$	t_1	t_2	t_3
$\phi =$	0.0°–22.5°	22.5°–45.0°	45.0°–67.5°
$D_1 =$	$K_1[I-(a_0+a)Q-aU+b_1V]$	$K_1[I-(a_0-a)Q-aU+b_2V]$	$K_1[I-(a_0-a)Q+aU+b_2V]$
$D_2 =$	$K_2[I+(a_0+a)Q+aU-b_1V]$	$K_2[I+(a_0-a)Q+aU-b_2V]$	$K_2[I+(a_0-a)Q-aU-b_2V]$

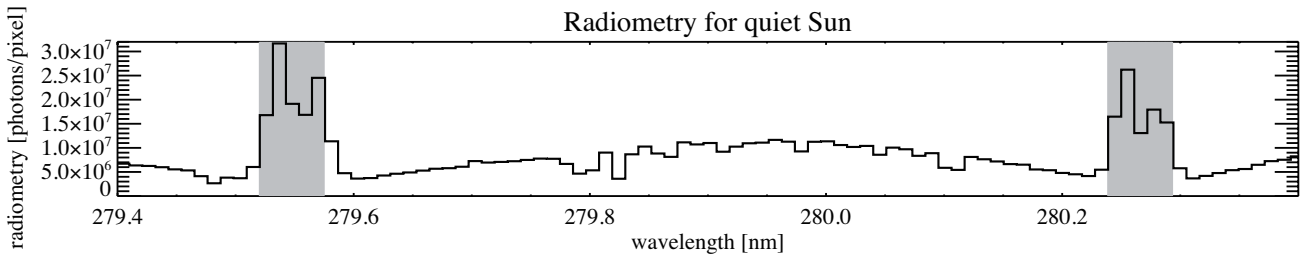

Figure 9. Predicted CLASP2 spectrum of the quiet Sun based on Mg II h & k spectra reported by.[23] The vertical axis is photons per detector pixel for total observing time of 231 sec (1.1 arcsec spatially and 0.011 nm in wavelength).

t_4	t_5	t_6
67.5°–90.0°	90.0°–112.5°	112.5°–135.0°
$K_1[I-(a_0+a)Q+aU+b_1V]$	$K_1[I-(a_0+a)Q-aU-b_1V]$	$K_1[I-(a_0+a)Q-aU-b_2V]$
$K_2[I+(a_0+a)Q-aU-b_1V]$	$K_2[I+(a_0+a)Q+aU+b_1V]$	$K_2[I+(a_0+a)Q+aU+b_2V]$

t_7	t_8	t_9	$\cdots$
135.0°–157.5°	157.5°–180.0°	180.0°–202.5°	$\cdots$
$K_1[I-(a_0-a)Q+aU-b_2V]$	$K_1[I-(a_0+a)Q+aU-b_1V]$	$K_1[I-(a_0+a)Q-aU+b_1V]$	$\cdots$
$K_2[I+(a_0-a)Q-aU+b_2V]$	$K_2[I+(a_0+a)Q-aU+b_1V]$	$K_2[I+(a_0+a)Q+aU-b_1V]$	$\cdots$

where K_1 and K_2 are throughput values of channels 1 and 2, D_1 and D_2 are the observed data values in these two channels, and ϕ is the rotation angle of the waveplate. Here we define the parallel to the slit as the positive reference direction for Stokes $+Q$. The modulation coefficients ($a_0 = 0.20$, $a = 0.51$, $b_1 = 0.30$, and $b_2 = 0.72$) represent the reduction in modulation that results from the continuous motion of the waveplate with the phase retardation of 127°. However, the improved S/N ratio that results from the continuous rotation and continuous exposure makes up for the reduced modulation, and achieves a higher polarizer sensitivity overall.

3.2.2 Demodulation

All the raw data are returned without onboard processing, and demodulation will be done on the ground using all flight data. First, we derive fractional polarizations (Q/I, U/I and V/I) using only the data from a single channel. For example, Q/I, U/I, and V/I are calculated from channel 1 data as:

$$\frac{Q}{I} = a^{-1} \times \frac{(-D_{1,t_1}+D_{1,t_2}+D_{1,t_3}-D_{1,t_4}-D_{1,t_5}+D_{1,t_6}+D_{1,t_7}-D_{1,t_8})+\cdots}{(D_{1,t_1}+D_{1,t_2}+D_{1,t_3}+D_{1,t_4}+D_{1,t_5}+D_{1,t_6}+D_{1,t_7}+D_{1,t_8})+\cdots}, \tag{1}$$

$$\frac{U}{I} = a^{-1} \times \frac{(-D_{1,t_2}+D_{1,t_3}+D_{1,t_4}-D_{1,t_5}-D_{1,t_6}+D_{1,t_7}+D_{1,t_8}-D_{1,t_9})+\cdots}{(D_{1,t_2}+D_{1,t_3}+D_{1,t_4}+D_{1,t_5}+D_{1,t_6}+D_{1,t_7}+D_{1,t_8}+D_{1,t_9})+\cdots}, \tag{2}$$

$$\frac{V}{I} = \left(\frac{b_1+b_2}{2}\right)^{-1} \times \frac{(D_{1,t_1}+D_{1,t_2}+D_{1,t_3}+D_{1,t_4}-D_{1,t_5}-D_{1,t_6}-D_{1,t_7}-D_{1,t_8})+\cdots}{(D_{1,t_1}+D_{1,t_2}+D_{1,t_3}+D_{1,t_4}+D_{1,t_5}+D_{1,t_6}+D_{1,t_7}+D_{1,t_8})+\cdots}, \tag{3}$$

with $Q \ll I$. Every successive set of 16 images of the data, corresponding to one rotation of the waveplate, will cancel out non-uniformities in the waveplate and fringe patterns caused by the waveplate. The Stokes signals from one channel will be verified by comparing to those from the other channel, and both signals will be summed to obtain the final Stokes profiles. This cancels possible polarization errors in the single-channel demodulation caused by time variation of source intensity and time variation of instrument pointing since two channels take orthogonal pairs of polarization simultaneously.[13,22] The alignment between two channels and the calibration of the throughput ratio between two channels will be performed using the flight data, essentially by summing all data in each channel.

3.3 Radiometry and Polarization Sensitivity

Prior to the first flight, we have investigated possible causes and expected magnitudes of polarization errors as shown in Table 3 of Ref. 24. The items to cause the spurious polarization remain the same and the magnitude of each error for CLASP2 will be similar to that for CLASP1. Referring to this table, by performing the dual-channel demodulation (see Section 3.2.2), the photon noise is the most important factor limiting the polarization sensitivity. Thus, predicting and verifying the polarization sensitivity requires accurate estimates of instrument

Table 2. Estimated CLASP2 throughput at MgII h&k.

component	material and thickness (t)	Channel 1	Channel 2
primary mirror	with cold mirror coating	> 90 %$^{(1)}$ [R]	
secondary mirror	with Al+MgF_2 coating	90 %$^{(2)}$ [R]	
waveplate	MgF_2, $t = 1$ mm	95 %$^{(3)}$ [T]	
grating	with Al+MgF_2 coating	29 %$^{(4)}$ [R]	
camera mirror	with Al+MgF_2 coating	90 %$^{(2)}$ [R]	
polarization analyzer	with multilayer coating (AOI = 68°)	75 %$^{(5)}$ [R_s]	
back-illuminated CCD	with Lumogen-E coating	30 %$^{(6)}$ [Q]	
throughput		4.5 %	

$^{(1)}$: Catalog value provided by Acton Optics & Coatings. $^{(2)}$: Our measured values at the UVSOR synchrotron facility. $^{(3)}$: Estimated value using optical index of MgF_2 at 280 nm. $^{(4)}$: Assuming the reflectivity of CLASP flight grating at Lyman-α line measured by the supplier (HORIBA Jobin Yvon). $^{(5)}$: Simulated value for multi-layer coating (Figure 7). $^{(6)}$: Based on the catalog value provided by Acton Optics & Coatings and our measurement. [R]: Reflectivity. [R_s]: [T]: Transmissivity. [Q]: Quantum efficiency.

throughput. We have been measuring the throughput for some of the components at UVSOR, and provide conservative estimates for those not tested in our facility (Table 2). The estimated values will be replaced by the measured value. We will also measure the reflectivity for the witness samples of flight coating at several times to monitor the aging, and keep this throughput table updated. Through the measurements for the throughput control for the first flight (CLASP), testing procedures are already established.

Based on the radiometry estimation, it is found that the number of photons collected for the shortest achievable exposure time of 0.1 sec is much larger than the peak charge storage of our CCDs. Therefore, we will place a Neutral Density (ND) filter with the transmissivity of 5% in order to maintain the linearity even with the observation of a plage region. The location is to be determined but we will choose the place where we can easily access as the transmissivity of the ND filter can be determined after throughputs of all optical components are actually measured. Figure 9 shows the predicted detectable flux over the observing time of 231 sec in the quiet Sun. The photon noises* of $\lesssim$0.05% around the Mg II h and k cores (gray regions in Figure 9), are achievable without spatial summation, and our requirement of polarization sensitivity can be met at $\sim 2\sigma$ level.

The level of visible light contamination was measured with the CLASP flight instrument using a heliostat at the NAOJ clean room. With this measurement, the predominant visible contamination path was identified and the contamination was suppressed to $\lesssim$100 photons/pixel/sec with the careful design of light traps and baffles. For the second flight, we will use the same structures and the contamination will be less than 0.1% of the expected Mg II peak signal.

4. SUMMARY

The measurement of the magnetic field vector in the solar outer atmosphere (chromosphere, transition region and corona) is a very important challenge in heliophysics. The most promising diagnostic tool for mapping the magnetic fields of the solar chromosphere and above is spectropolarimetry in UV lines, which requires the deployment of a UV polarimeter in space. CLASP, which will fly in September 2015, will measure the linear polarization signals in the Lyman-α line and will provide the first quantitative exploration of the magnetic field in the solar upper chromosphere and transition region via the Hanle effect. *The proposed Chromospheric LAyer Spectro-Polarimeter (CLASP2) is the natural next step.* CLASP2 will measure the linear and circular polarization signals in the Mg II h and k lines in order to study the magnetic field vector in the upper solar

*The photon noise is estimated from $1/a/\sqrt{N}$, where N is the total number of photons to be collected and a the modulation coefficient. See Ref. 24 for more detail.

chromosphere by combing the Hanle and Zeeman effects. Moreover, these measurements coordinated with those of IRIS, will lead to significant quantitative insight on the enigmatic solar chromosphere, such as refining the theoretical models of chromospheric jets and the dissipation mechanism of magnetic energy in the chromosphere and corona. CLASP2 will target a high priority science question recommended by the Heliophysics Roadmap, "What is the magnetic structure of the Sun-heliosphere system?", by measuring the magnetic field in a crucial boundary layer, the upper solar chromosphere.

Exploring the magnetism of the upper chromosphere through spectropolarimetric measurements of the Zeeman and Hanle effects in UV spectral lines is an important future direction for solar physics. CLASP2 will serve as a pathfinder for future solar missions. The CLASP2 program is also training the next generation of instrument builders by involving young scientists in optical design and testing from the beginning to the end of the program.

ACKNOWLEDGMENTS

The authors acknowledge all members of the Chromospheric Lyman-Alpha SpectroPolarimeter (CLASP) team. The team is an international partnership between NASA Marshall Space Flight Center and JAXA; additional partners include National Astronomical Observatory of Japan, Kyoto University, National Institute for Fusion Science, Instituto de Astrofisica de Canarias, Institut d'Astrophysique Spatiale, Le Centre national d'études spatiales, the University of Alabama in Huntsville, Lockheed Martin, High Altitude Observatory, and Universitetet i Oslo. The development of the high reflectivity polarizing coating was supported by the Japan Society for the Promotion of Science (JSPS) through a Grant-in-Aid for Young Scientists (B) (Grant Number 24740134, PI: N. Narukage) and the basic research program of the Institute of Space and Astronomical Science (ISAS) (PI: N. Narukage). The development of the reflective narrow band filter coating and the high reflectivity mirror coating was supported by JSPS through Scientific Research (S) (Grant Number 25220703, PI: S. Tsuneta) and (B) (Grant Number 24340040, PI: R. Kano), and the internal research funding of the National Astronomical Observatory of Japan (NAOJ). We acknowledge M. Hasumoto and K. Tanaka at the Institute for Molecular Science, S. Kimura at Osaka University, and K. Fukui at Fukui University for their support of our experiment at Ultraviolet Synchrotron Orbital Radiation Facility (UVSOR).

REFERENCES

[1] Belluzzi, L. and Trujillo Bueno, J., "The Polarization of the Solar Mg II h and k Lines," ApJ **750**, L11 (May 2012).

[2] Trujillo Bueno, J., Štěpán, J., and Casini, R., "The Hanle Effect of the Hydrogen Lyα Line for Probing the Magnetism of the Solar Transition Region," ApJ **738**, L11 (Sept. 2011).

[3] Trujillo Bueno, J., Štěpán, J., and Belluzzi, L., "The Lyα Lines of H I and He II: A Differential Hanle Effect for Exploring the Magnetism of the Solar Transition Region," ApJ **746**, L9 (Feb. 2012).

[4] Belluzzi, L., Trujillo Bueno, J., and Štěpán, J., "The Scattering Polarization of the Lyα Lines of H I and He II Taking into Account Partial Frequency Redistribution and J-state Interference Effects," ApJ **755**, L2 (Aug. 2012).

[5] Štěpán, J., Trujillo Bueno, J., Leenaarts, J., and Carlsson, M., "Three-dimensional Radiative Transfer Simulations of the Scattering Polarization of the Hydrogen Lyα Line in a Magnetohydrodynamic Model of the Chromosphere–Corona Transition Region," ApJ **803**, 65 (Apr. 2015).

[6] Hanle, W., "Uber magnetische Beeinflussung der Polarisation der Resonanzfluoreszenz," *Z. Phys* **30**, 93–105 (1924).

[7] Ishikawa, R., Asensio Ramos, A., Belluzzi, L., Manso Sainz, R., Štěpán, J., Trujillo Bueno, J., Goto, M., and Tsuneta, S., "On the Inversion of the Scattering Polarization and the Hanle Effect Signals in the Hydrogen Lyα Line," ApJ **787**, 159 (June 2014).

[8] Štěpán, J. and Trujillo Bueno, J., "PORTA: A three-dimensional multilevel radiative transfer code for modeling the intensity and polarization of spectral lines with massively parallel computers," A&A **557**, A143 (Sept. 2013).

[9] Belluzzi, L. and Trujillo Bueno, J., "The transfer of resonance line polarization with partial frequency redistribution and J-state interference. Theoretical approach and numerical methods," A&A **564**, A16 (Apr. 2014).

[10] Martínez-Sykora, J., De Pontieu, B., and Hansteen, V., "Two-dimensional Radiative Magnetohydrodynamic Simulations of the Importance of Partial Ionization in the Chromosphere," ApJ **753**, 161 (July 2012).

[11] Centeno, R., Trujillo Bueno, J., and Asensio Ramos, A., "On the Magnetic Field of Off-limb Spicules," ApJ **708**, 1579–1584 (Jan. 2010).

[12] Judge, P., "Observations of the Solar Chromosphere," in [*Solar MHD Theory and Observations: A High Spatial Resolution Perspective*], J. Leibacher, R. F. Stein, & H. Uitenbroek, ed., *Astronomical Society of the Pacific Conference Series* **354**, 259 (Dec. 2006).

[13] Narukage, N., Auchère, F., Ishikawa, R., Kano, R., Tsuneta, S., Winebarger, A. R., and Kobayashi, K., "Vacuum ultraviolet spectropolarimeter design for precise polarization measurements," Appl. Opt. **54**, 2080 (Mar. 2015).

[14] West, E. A., Porter, J. G., Davis, J. M., Gary, G. A., Noble, M. W., Lewis, M., and Thomas, R. J., "The Marshall Space Flight Center solar ultraviolet magnetograph," in [*Society of Photo-Optical Instrumentation Engineers (SPIE) Conference Series*], G. Hasinger & M. J. L. Turner, ed., *Society of Photo-Optical Instrumentation Engineers (SPIE) Conference Series* **5488**, 801–812 (Oct. 2004).

[15] Podgorski, W. A., Cheimets, P. N., Golub, L., Lemen, J. R., and Title, A. M., "Design, performance prediction, and measurements of the interface region imaging spectrograph (IRIS) telescope," in [*Space Telescopes and Instrumentation 2012: Ultraviolet to Gamma Ray. Proceedings of the SPIE*], Takahashi, T., Murray, S. S., and den Herder, J.-W. A., eds., 84433D–84433D–11, Harvard-Smithsonian Ctr. for Astrophysics (United States), SPIE (Sept. 2012).

[16] Giono, G., Ishikawa, R., Narukage, N., Kano, R., Katsukawa, Y., Kubo, M., Ishikawa, S., Bando, T., Hara, H., Suematsu, Y., Winebarger, A. R., Kobayashi, K., Auchère, F., and Trujillo-Bueno, J., "CLASP polarization calibration: Reaching below the 0.1% polarization sensitivity in the VUV range," Sol. Phys. **in preparation** (2015).

[17] Watanabe, H., Narukage, N., Kubo, M., Ishikawa, R., Bando, T., Kano, R., Tsuneta, S., Kobayashi, K., Ichimoto, K., and Trujillo-Bueno, J., "Ly-alpha polarimeter design for CLASP rocket experiment," in [*Society of Photo-Optical Instrumentation Engineers (SPIE) Conference Series*], *Society of Photo-Optical Instrumentation Engineers (SPIE) Conference Series* **8148** (Sept. 2011).

[18] Palik, E. D., [*Handbook of optical constants of solids*] (1985).

[19] Ishikawa, R., Kano, R., Bando, T., Suematsu, Y., Ishikawa, S.-n., Kubo, M., Narukage, N., Hara, H., Tsuneta, S., Watanabe, H., Ichimoto, K., Aoki, K., and Miyagawa, K., "Birefringence of magnesium fluoride in the vacuum ultraviolet and application to a half-waveplate," Appl. Opt. **52**, 8205 (Dec. 2013).

[20] Ishikawa, S., Shimizu, S., Kano, R., Bando, T., Ishikawa, R., Giono, G., Tsuneta, S., Nakayama, S., and Tajima, T., "Development of precise polarization modulator for UV spectropolarimetry," Sol. Phys. **in press** (2015).

[21] Bridou, F., Cuniot-Ponsard, M., Desvignes, J.-M., Gottwald, A., Kroth, U., and Richter, M., "Polarizing and non-polarizing mirrors for the hydrogen Lyman- α radiation at 121.6 nm," *Applied Physics A: Materials Science & Processing* **102**, 641–649 (Mar. 2011).

[22] del Toro Iniesta, J. C., [*Introduction to Spectropolarimetry*] (May 2007).

[23] Allen, M. S., McAllister, H. C., and Jefferies, J. T., "High resolution atlas of the solar spectrum 2678-2931 A," *NASA STI/Recon Technical Report N* **78**, 31029 (1977).

[24] Ishikawa, R., Narukage, N., Kubo, M., Ishikawa, S., Kano, R., and Tsuneta, S., "Strategy for Realizing High-Precision VUV Spectro-Polarimeter," *Solar Physics* **289**, 4727–4747 (Dec. 2014).